Effect of Plasma Plume on CubeSat Structures as a Function of Thrust Vectoring

Presented at Joint Conference of 30th International Symposium on Space Technology and Science 34th International Electric Propulsion Conference and 6th Nano-satellite Symposium, Hyogo-Kobe, Japan July 4 – 10, 2015

Andrew D. Hine[1] and Kristina M. Lemmer[2]
Western Michigan University, Kalamazoo, MI, 49009, United States of America

Abstract: This paper details research studying the integration of electric propulsion devices on CubeSats. The research examined how the presence of an electric propulsion device could affect nominal spacecraft operation and long term degradation of the spacecraft structure. This was accomplished by examining the plasma plume of a 1 cm gridded Kauffman style ion source, where the presence of low energy ions that may indicate high-energy neutrals near the spacecraft and within the plume was investigated. The existence of high-energy neutrals in close proximity to a spacecraft structure could result in the degradation of the structure and subsystems. When implementing electric propulsion devices on spacecraft this is an important characteristic to understand and must be taken into account during integration. Ion energy measured using a retarding potential analyzer shows that there are low-energy ions outside of the plasma plume of a gridded ion source. Faraday probe results for thrust vectoring show that the bulk of the plasma plume is oriented at the same angle as the vectored thruster.

Nomenclature

A_c	=	Area of RPA collector
e	=	Charge on an electron
I	=	Current
m_i	=	Mass of an ion
n_i	=	Ion number density
V	=	Voltage
V_a	=	Actual measured voltage
V_{mp}	=	Most probable ion voltage
V_p	=	Plasma potential
Z_i	=	Charge state of the ions

I. Introduction

THE growing interest in CubeSat propulsion has motivated the development of many micro propulsion devices.[1] These propulsion devices will require some sort of active control strategy to become mission ready.[2] One potential control approach is to use thrust vectoring to allow the primary propulsion system to also act as the attitude control system. To evaluate the potential success of such a system, functional testing of thrust vectoring limits for CubeSats must be completed. Implementing electric propulsion devices onto CubeSats presents many unique challenges for the propulsion system. For example, mission critical payload components and the propulsion system must function within close proximity to each other while maintaining long-term operation. All potential interactions

[1] Graduate Research Assistant, Department of Mechanical and Aerospace Engineering, andrew.d.hine@wmich.edu.
[2] Assistant Professor, Department of Mechanical and Aerospace Engineering, kristina.lemmer@wmich.edu.

between these systems must be well characterized to ensure limited long-term system degradation due to unwanted interaction between the thruster plume and spacecraft subsystems. This work seeks to understand the relationship between the spacecraft and plasma plume and characterize the potential for unwanted spacecraft-plasma interactions. Further understanding of thrust-vectoring limits will help define the maneuvering capabilities of future CubeSat propulsion missions.

The purpose of this project is to determine the extent to which thrust vectoring on a CubeSat will affect the satellite body and how much the thruster can be vectored before the plasma plume impinges on the CubeSat. To accomplish this, a thruster plume was created using a 1-cm-diameter gridded ion source operating with Xenon. Faraday probe and a retarding potential analyzer (RPA) data were obtained as a function of radial distance from and angle to the thruster exit to evaluate the plume characteristics of the thruster. To simulate thrust vectoring on a spacecraft the ion source was oriented at three angular directions to a simulated spacecraft axis: 0°, 2.5°, and 5°.

II. Experimental Setup

All testing was performed at the Aerospace Laboratory for Plasma Experiments (ALPE) at Western Michigan University. The vacuum facility is a 1.22-m-diameter by 1.83-m-long stainless steel vacuum chamber with a pumping capacity of 1050 l/s nitrogen. The vacuum chamber base pressure can reach 5E-7 torr. A Penning Magnetron Cold Cathode gauge with an accuracy of ±0.2 decades within its operating range of 1.0E-7 to 1.0E-3 torr was used to measure chamber pressure.

A. Ion Source

To produce an ion thruster plume, a 1-cm gridded Kauffman and Robinson ion source was used. The source produced an ion beam with a 400 V potential and a beam current of 10 mA. The ion source was controlled by a Kaufman Source Power Supply Controller and operated with 1.8 sccm of Xenon. The flow rate was controlled with an Alicat mass flow controller, and the vacuum chamber background operating pressure was 1.6E-4 torr. Table 1 summarizes the average ion source operating conditions. The ion source was installed in the vacuum facility with the ability to rotate the direction of the plume about the center of the ion source grid face. Figure 1 shows a schematic and a photograph of the experimental setup.

Table 1. Nominal Operating Conditions of Ion Source

Cathode		Discharge		Beam		Accel		Neutralizer		
Voltage (V)	Current (A)	Voltage (V)	Current (A)	Voltage (V)	Current (mA)	Voltage (V)	Current (mA)	Emission (mA)	Voltage (V)	Current (A)
3.9	5.85	40	0.27	400	10	90	1.8	8	4.2	10.3

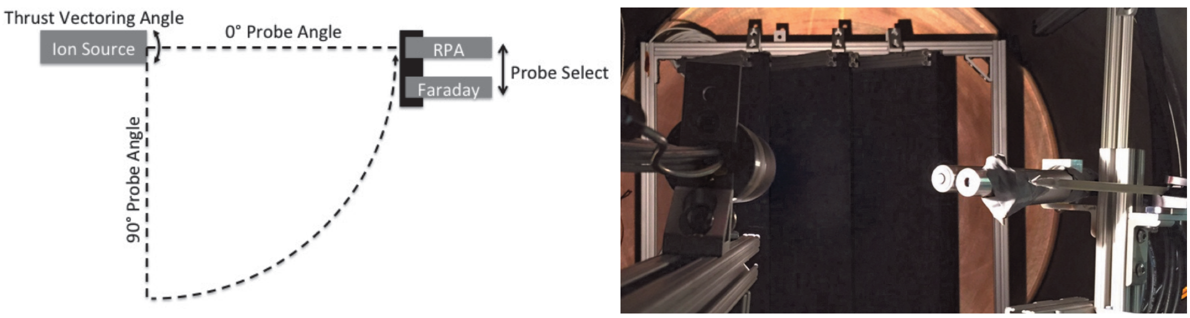

Figure 1. Experimental Setup. *Shown are a diagram (left) and photograph (right) of the experimental setup with the ion source, Faraday probe, and RPA. The ion source was rotated about the centerline of its exit, and the probes were on linear and rotation tables to allow sweeps of the plasma plume.*

B. Plasma Diagnostics

Properties of the ion source plume were measured with two plasma probes: a Faraday probe and an RPA. The probes were secured to motion control tables and swept through the plasma plume at varying angles and radii from the ion source. Faraday probe measurements were obtained for the 0°, 2.5°, and 5° thrust vector angles at radial distances of 31.75 mm, 56.75 mm, 81.75 mm, 106.75 mm, 141.75 mm, and 171.75 mm from the center of the ion source face. The Faraday probe measured current at 1° increments throughout the plasma plume. RPA data were collected only when the ion source was aligned at the 0° thrust vectoring angle and were measured at radial distances of 31.75 mm, 106.75 mm, and 171.75 mm from the ion source at 5° angular increments through the plasma plume.

A nude, nested faraday probe was used to measure the ion beam current density from the gridded ion source to a negatively biased collector. The faraday probe consists of two concentric electrodes that are biased to -15V to repel low mass electrons while keeping the affect on the more massive ions negligible. Current is measured from the central electrode, while the outer electrode is used to create a flat potential profile.[3] The collected current values are divided by the area of the inner electrode. This calculation gives a measure of the ion current density in the plume. A diagram of the nested Faraday probe used for this project is presented in Figure 2.[3]

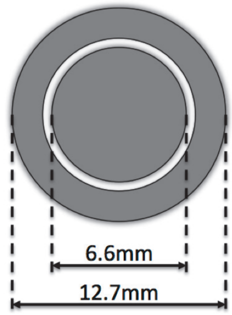

Figure 2. Faraday Probe Diagram. *Nested Faraday probe that was used to measure ion current density in the plume of the gridded ion source*

A retarding potential analyzer (RPA) was used to determine the ion energy distribution function (IEDF) at set locations within the ion source plume. The RPA was built with four charged grids (Figure 3), spaced 1 mm apart, and aligned behind a 6.22 mm orifice through which the plasma enters. Upon entering the RPA, the particles encounter a series of grids and are filtered by their ion energy.[5] The first grid is the neutralizer, and it is electrically floating to minimize plasma perturbations. The second grid is the electron repelling grid, and it is biased to -60 V to repel incoming electrons. The third grid is the ion retarding grid. A controlled varying voltage from 0 to 450 V is applied to the ion retarding grid so that as the voltage on the grid is increased, ions are filtered by their energy-to-charge ratios. The final grid is the electron suppression grid, and it is held at -13 V to repel any secondary electrons that may have been created through collisions within the probe itself. The final component of the RPA is the collector. The current to the collector as a function of the ion retarding grid potential was measured throughout the ion source plume

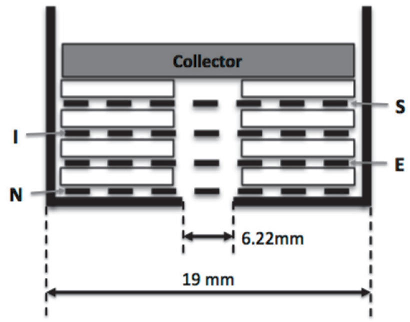

Figure 3. RPA Diagram. *The RPA was a 4-grid design with E = electron repelling grid, I = ion retarding grid, S = electron suppression grid, and N = neutralizing grid*

III. Data Analysis

Current to the inner electrode of the Faraday probe was recorded at the previously discussed downstream locations in the ion source plume using a LabView VI. Current density was calculated using the area of the inner electrode, and it was normalized for each thrust vectoring position of the ion source for comparison. Using Tecplot, the normalized current density data were triangulated, and contour plots of normalized current density vs. downstream location were produced. Faraday probe uncertainties can arise for a number of reasons. One reason is because the effective probe collection area decreased as the probe was rotated away from the centerline of the plasma plume. Additionally, the size of the probe collection area influences the resolution of the collected data. Keeping the Faraday probe small is ideal; however, that must be balanced with collecting a measurable current. Facility effects for far field measurements can also contribute to uncertainties due to the collection of facility low energy charge exchange collision ions.[4]

The RPA current-voltage characteristic was recorded using a LabView VI at each radius and angular position. The collected current-voltage data were saved in a spreadsheet format and imported into MatLab for analysis. The raw collected data points were then smoothed using a moving average over a span of 25 points. The smoothed data were used to create a piecewise polynomial spline fit in MatLab. The derivative of the current-voltage characteristic is proportional to the ion energy distribution function (IEDF), as shown in Eq. 1.[5]

$$\frac{dI}{dV} = -\frac{e^2 Z_i^2 n_i A_c}{m_i} f(V) \propto -f(V) \tag{1}$$

The IEDF was determined by taking the derivative of the spline fit polynomial with respect to the voltage applied to the probe using the central difference quotient method.

$$\frac{df}{dx} = \frac{f(x+\Delta x) - f(x-\Delta x)}{2\Delta x} \quad (2)$$

The IEDF was normalized to unity to facilitate comparison between data points. The most probable ion energy is the potential where the peak of the IEDF occurs.[6] For some locations around the plasma plume, there is more than a single peak, indicating the presence of ions at more than one probable energy level. Figure 6 shows an example current vs. voltage trace, the resulting smoothed data and spline fit curve, and the normalized IEDF.

The ion retarding grid potential is applied with respect to facility ground, so the ion energy-per-charge must be corrected for the plasma potential:

$$V_a = V_{mp} + V_p \quad (3)$$

Any variations from the set ion source beam potential of 400 V are due to the plasma potential. Other uncertainties in RPA measurements come from having insufficient voltage applied to the electron or ion repelling grids.[6]

IV. Experimental Data

A. Faraday Probe

Faraday probe data were measured at three vectoring angles of the ion source. Figure 4 shows the contour plots of the normalized ion current density in the plasma plume generated by the ion source as a function of downstream position and ion source vectoring angle. The contour plots show a dip in the current density along the axial centerline of the ion source. This indicates that the center of the plasma plume has fewer ions than the edges. This is unexpected in a gridded ion source and is indicative of more plasma formed and accelerated at the edges of the ion source than in the middle. This may be because of the simplicity of the Kauffmann-style ion source magnetic field.[7] The angle of the plasma plume, as indicated by the highest current density in the contour plots, aligns with the thrust vectoring angle within measurement errors. When the ion source is angled at 2.5° from the spacecraft centerline, the line of maximum current density is 3.5° from the same line at 0° ion source vector angle. This is seen in Figure 4. The same trend is apparent at the 5° vector angle where the angle between the two lines of maximum current density is 6°. Another trend that can be seen from Figure 4 is that the bulk of the plasma plume remains at angles close to the thruster centerline. This is a good indication that the plasma will not impinge significantly on spacecraft surfaces.

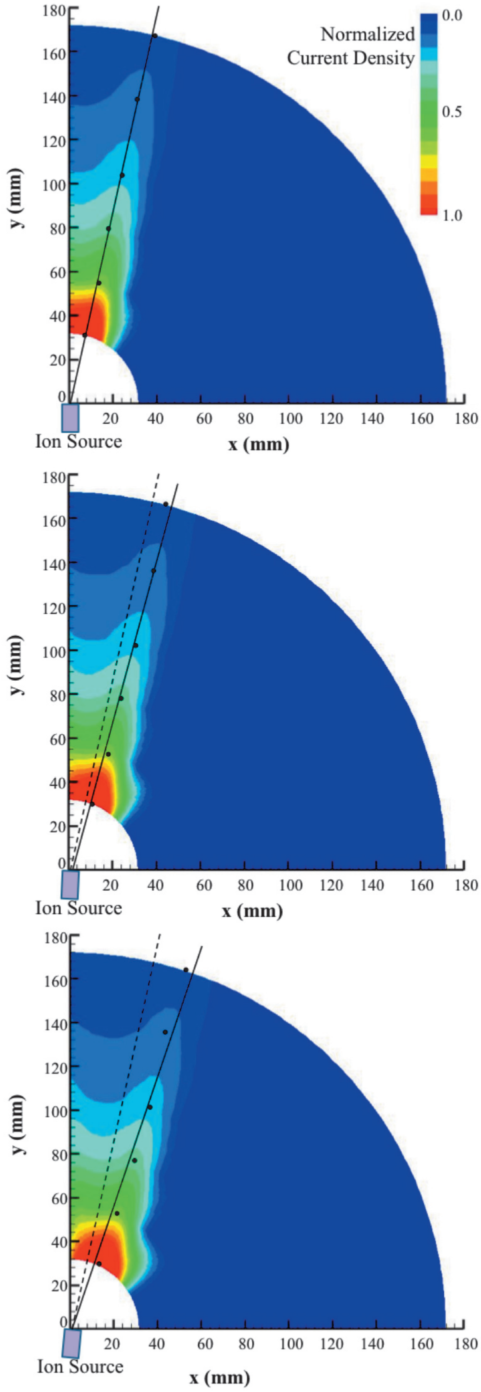

Figure 4. Normalized ion current density for three thrust vectoring angles: 0° (top), 2.5° (middle), and 5° (bottom). *Normalized current density was triangulated between radial and angular data points to produce contour plots. Indicated on each plot is the 0° line of highest current density, and for 2.5° and 5° plots, their line of highest current density.*

B. RPA

RPA data give the most probable ion energy as a function of plasma plume location. For locations near to the ion source axial centerline, the most probable ion energy is the beam voltage offset by the plasma potential, as expected. The most probable ion energy as a function of downstream location is plotted in Figure 5. In the regions near 90° from the ion source axial centerline, there are low energy ions at about 15 V. In the plume regions between axial and perpendicular (between 20° and 60°), both 15 V and 400 V ions exist. Closer to the ion source exit at shorter radial distances to the ion source grids ions with a broad range of energies exist.

Figure 6 shows sample RPA traces, the corresponding smoothed data, and the IEDF for locations where only 400 V ions exist (left), both 400 V and 15 V ions exist (center), and only 15 V ions exist (right) The scales on each plot are normalized to their own maximum, but the maximum values differ significantly between each location. The maximum current at 5° is an order of magnitude higher than the maximum current at 40° which is an order of magnitude higher than the maximum current at 85°. The presence of the low energy ions in the regions perpendicular to the ion source axial centerline indicate that there may be higher energy neutrals due to charge-exchange collisions. Charge exchange collisions result when a high-energy ion impacts a low energy neutral, and an electron transfers from the ion to the neutral.[8] With the charge exchange, the high-energy ion becomes a high energy neutral. The high energy neutral cannot be controlled by any electric or magnetic fields, and can cause significant damage to the spacecraft. However, because the current collected outside of the ion source plume is two orders of magnitude less than that the plume itself, the actual damage may be minimal.

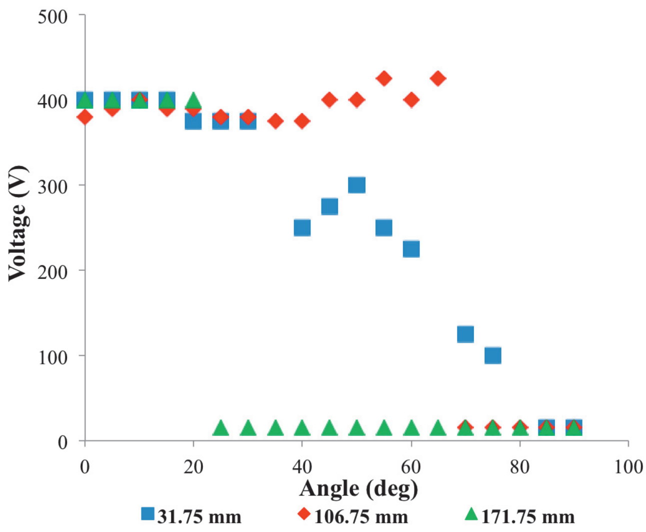

Figure 5. Most probable ion voltage vs. location in plasma plume along the axial centerline of the ion source. *The most probable ion voltage is the expected beam voltage of 400 V. At locations near 90° from the ion source axis, the most probable ion voltage is around 15 V. Between, there are regions where both 400 V and 15 V ions are present.*

V. Conclusion and Future Work

Limited beam divergence was found within the plasma plume of a gridded Kauffman-style ion source. The Faraday probe data show the high energy plasma plume with little divergence as it moves downstream from the spacecraft structure. The RPA data do show evidence of possible high energy neutrals at high divergence angles away from the ion source centerline. Further investigation is needed to measure the density of the low energy ions near the spacecraft surface. This will give an indication of the quantity of high energy neutrals near a spacecraft. The use of optical emission spectroscopy could also be useful to determine the number of high energy neutrals near a spacecraft surface by measuring the emission intensity of neutral Xenon.[9] Future work includes repeating the experiments using a micro thruster designed for a CubeSat type spacecraft, specifically an RF, gridded ion thruster. In these upcoming experiments the number of probe sweeps will be increased to include a greater number of radial distances around the thruster to better characterize its plume. Adding a Langmuir probe will allow for the calculation of ion number density, providing further insight. Running these experiments with the RF thruster installed in a simulated CubeSat structure will help to identify pertinent integration issues between an electric propulsion thruster and CubeSat subsystems.

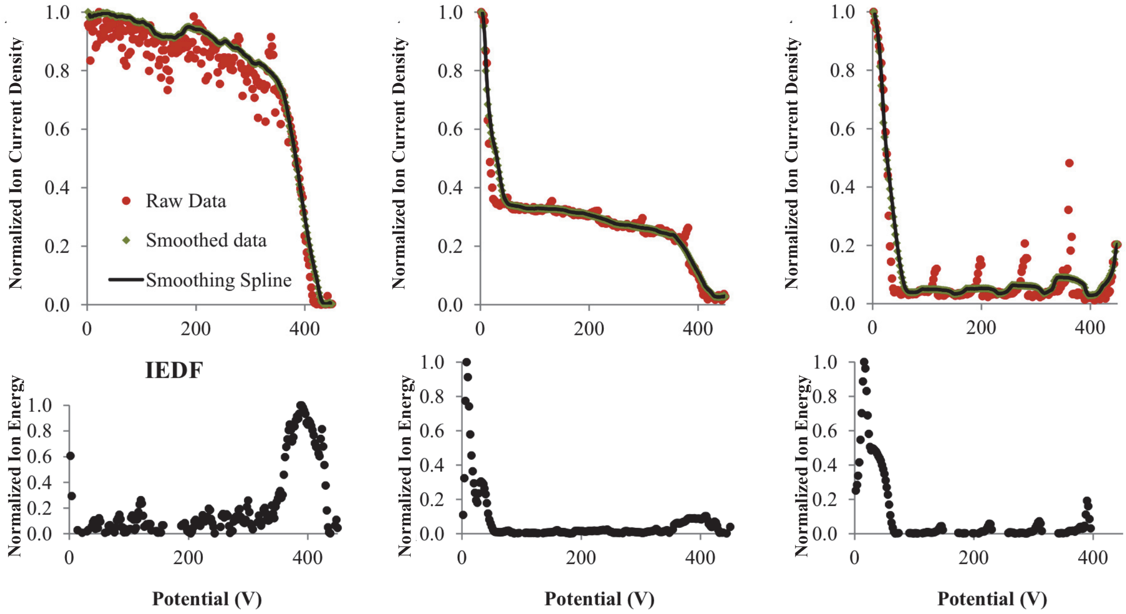

Figure 6. RPA characteristics at three locations within the plasma plume. *All characteristics were measured at 171.75 mm radial distance from the ion source face with the ion source at 0° vector. Left: 5° from the ion source axial centerline where the most probable ion energy is 400V. Center: 40° from the ion source axial centerline where there are ions at 15 V and 400 V. Right: 85° from the ion source axial centerline where the most probable ion energy is15V. Note that all pots are normalized to their own maximum value.*

Acknowledgments

The authors would like to thank the NASA Small Spacecraft Technology Program and Space Technology Mission Directorate (STMD) for their support of this research.

References

[1] Mueller, J., Hofer, R. and Ziemer, J., "A Survey on Propulsion Technologies Applicable to CubeSats," *Joint Army-Navy-NASA-Air Force (JANNAF)*, Vol. 1, Pasadena, CA, National Aeronautics and Space Administration, 2010.

[2] Kolosa, D., Spangelo, S. Lemmer and K. Husdson, J., "Mission Analysis for a Micro RF Ion Thruster for CubeSat Orbital Maneuvers," *50th AIAA/ASME/SAE/ASEE Joint Propulsion Conference*, 2014.

[3] Brown, D., "Investigation of Low Discharge Voltage Hall Thruster Characteristics and Evaluation of Loss Mechanisms," Ph.D., Dissertation, Aerospace Engineering, University of Michigan, Ann Arbor, MI, 2009.

[4] Walker, M., Victor, A., Hofer, R., and Gallimore, A., "Effect of Backpressure on Ion Current Density Measurements in Hall Thruster Plumes," *Journal of Propulsion and Power*, Vol. 21, No. 3 (2005), pp. 408-415.
doi: 10.2514/1.7713

[5] Hutchinson, I. H., *Principles of Plasma Diagnostics*. 2nd ed., Cambridge University Press,2002..

[6] Lemmer, K. M., "Use of a Helicon Source for Development of a Re-Entry Blackout Amelioration System," Ph.D. Dissertation, Aerospace Engineering, University of Michigan, Ann Arbor, MI, 2009.

[7] Goebel, D. and Katz, I., *Fundamentals of Electric Propulsion: Ion and Hall Thrusters,* John Wiley and Sons, New Jersey, 2008

[8] Bellan, P. *Fundamental of Plasma Physics,* Cambridge University Press, New York, 2006

[9] Sengupta, A., Goebel, D. and Owens, A., "Neutral Density Measurements in an NSTAR Ion Thruster," *42nd AIAA/ASME/SAE/ASEE Joint Propulsion Conference*, 2006.